Thermo-electro-mechanical modeling of thermal fatigue failure process of corset samples from single-crystal nickel superalloys

Artem V. Savikovskii, Artem S. Semenov, Leonid B. Getsov
temachess@yandex.ru

Abstract

The results of computations of the thermal and stress-strain state of single-crystal corset specimens subjected to the action of periodic electric current, leading to variable inhomogeneous heating and subsequent thermal fatigue failure, are presented. The influence of maximum value and range of temperature and also delay time at the maximum temperature on the number of cycles before the macrocrack formation is investigated. Comparison of the computational results with the experimental data for various single-crystal nickel-based superalloys showed a good accuracy.

1 Introduction

Single-crystal nickel-based superalloys [1] are widely used for the manufacture of nozzle and working blades of gas turbine engines (GTE). The thermal-fatigue strength of such materials with a pronounced anisotropy and a sensitivity of mechanical properties to the temperature is currently not fully studied. For the investigation of thermal fatigue durability under a wide range of temperatures with and without intermediate delays the experiments are carried out on different types of samples, including corset (plane) specimen on the installation developed in NPO CKTI [2] (see Fig. 1 a). Fixed in axial direction by means of two bolts with a massive foundation the corset sample (see Fig. 1 b) is heated periodically by passing electric current through it. During cycling the maximum and minimum temperatures are automatically maintained constant.

The objective of the study is to determinate numerically the thermal and stress-strain states of the corselet specimens under cyclic electric loading and to study systematically the effect of delay at maximum temperature on the thermal fatigue durability on the base of the deformation criterion [3, 4, 5] of thermal-fatigue failure for single crystal superalloys using the results of finite element (FE) simulation of full-scale experiments. The results of simulation and their verification are obtained for the different single-crystal nickel-based superalloys: VZhM4, VIN3 and ZhS32.

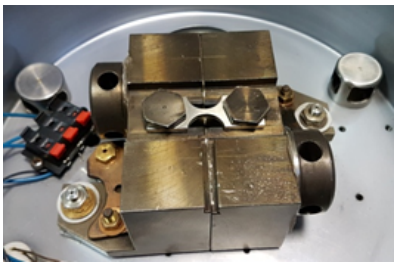
a)

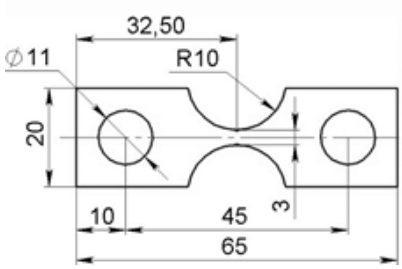

b)

Figure 1: a) Installation for carrying out experiments on thermal fatigue, b) Geometry corset sample for thermal fatigue experiment.

2 Results of thermo-electric analysis

Modeling of heating process in the corset samples was carried in the FE program ANSYS with taking into account the temperature dependence of all material properties, nonstationary Joule heating, the convective heat exchange and radiative heat transfer between the sample and the environment. The full-scale FE model of experimentation object including discrete models of the specimen and the setup is presented in Fig. 2.

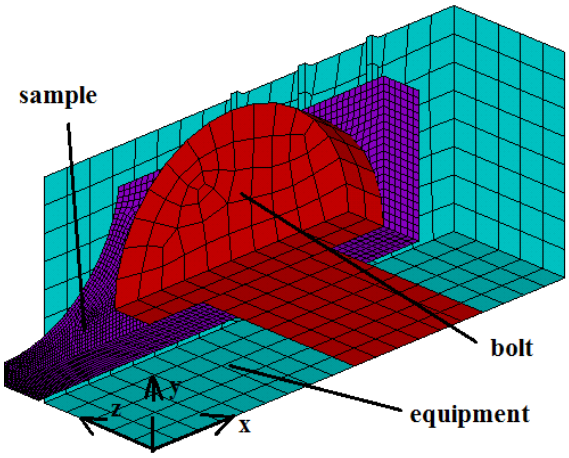

Figure 2: Finite-element model for thermoelectric problem.

Modeling of heating processes and thermal fatigue fracture of sample was carried out for four temperature regimes (modes): $150 \div 900$, $250 \div 1000$, $500 \div 1050$ and $700 \div 1050°C$. The used in FE simulations material properties for the single crystal nickel superalloy sample and for the steel equipment were taken from literature [6], [13, 14, 15] (see also Table 1). While specifying the properties of nickel alloy and steel the implementation of the Wiedemann-FranzвГЄs law was controlled: $\lambda\rho_e =$ LT, where λ is the thermal conductivity,ρ_e is the specific electrical resistance, T is the temperature in K, $L = 2.22 \cdot 10^{-8} W\Omega K^{-2}$ is the *Lorentz's* constant.

Table 1. Thermo-electric properties of nickel superalloy used in FE simulations.

T	$°C$	20	200	400	800	1000	1150	Ref.
ρ	$\frac{kg}{m^3}$	8550	8500	8450	8350	8330	8310	[13]
C_ρ	$\frac{J}{kg \cdot K}$	440	520	520	575	590	600	[13]
λ	$\frac{W}{m \cdot K}$	7.4	11.2	14.1	19.8	26.7	36.7	[6]
ρ_e	$\Omega \cdot m$	$8.7 \cdot 10^{-7}$	$9.3 \cdot 10^{-7}$	$1.1 \cdot 10^{-6}$	$1.2 \cdot 10^{-6}$	$1 \cdot 10^{-6}$	$8.9 \cdot 10^{-7}$	[6]

The coupled three-dimensional transient thermo-electrical analysis has been performed. Due to the symmetry in respect to the xz and yz planes, a quarter of the structure was considered. The thermal and electric contacts between the sample and bolts, between the sample and the foundation were taken into account. The initial temperature for the sample and the equipment was set to 30 $°C$. For the free surface of sample the boundary condition of convective heat transfer is used:

$$q_n = h(T - T_0), \tag{1}$$

where n is the normal to body, q_n is the heat flux density, $h = 20\frac{W}{m^2 K}$ is the coefficient of convective heattransfer, T_0 is the ambient temperature. The condition of radiative heat transfer was also set on the surfaces of central (high temperature) part of the sample (10 mm length):

$$q_n = \varepsilon \sigma_{SB}(T^4 - {T_0}^4), \tag{2}$$

where $\varepsilon = 0.8$ is the black factor of the body, $\sigma_{SB} = 5.67 \cdot 10^{-8} W m^{-2} K^{-4}$ is the coefficient of Stefan-Boltzmann.
The temperature field distribution in the VZhM4 sample is shown in Fig. 3a for the loading regime with $T_{max} = 1050°C$. Note that the solution of thermo-electric problem has been obtained for the complete FE model shown in Fig. 2 with taking into account the equipment.The evolution of temperature spatial-distribution is given in Fig. 3b (x is a distance from the sample center). The bell-form of the curve is keeping during whole heating process.

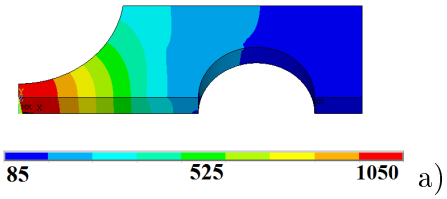

a)

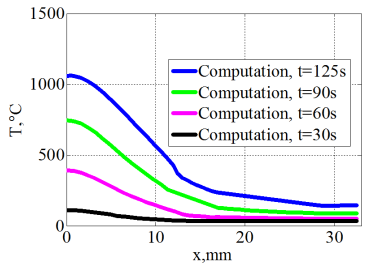

b)

Figure 3: a) Temperature field distributions in VZhM4 sample by heating for regime with $T_{max} = 900°C$, b) Evolution of temperature distribution along the VZhM4 sample axis for different heating times.

The comparison of FE results with experimental data for axial temperature distribution demonstrates a good agreement for the all considered loading regimes (see, for example, Fig. 4).

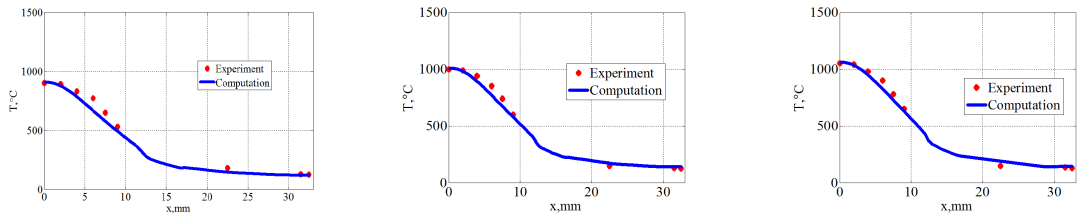

Figure 4: Comparison of computational results with experimental data for axial temperature distributions in VZhM4 sample for regimes with: a) $T_{max} = 900°C$,b) $T_{max} = 1000°C$, c) $T_{max} = 1050°C$

3 Results of thermo-elasto-visco-plastic analysis

The obtained in thermo-electric problem the spatial and temporal distribution of the temperature field is the base for the strain and stress field computation within the framework of thermo-elasto-visco-plastic problem solution.
The fixing of sample under heating leads to the high stress level and inelastic strain appearance. The local strain and stress concentration is observed in the central (working) part of sample. The FE simulation is required for the computation of inhomogeneous stress and inelastic strain fields. Modeling of inelastic deformation in the corset samples has been performed with taking into account of the temperature dependence of all material properties, anisotropy of mechanical properties of single crystal sample, kinematic hardening, inhomogeneous nonstationary temperature field, mechanical contacts bolt/specimen and specimen/foundation, friction between the contact surfaces, temperature expansion in the specimen, bolt and foundation. The two FE formulations for the thermo-mechanical problem have been considered:

- with taking into account of equipment;
- without taking into account equipment (simplified formulation [7] for the sample only).

Using the second formulation provides significant saving computational time due to reduction in the number of degrees of freedom and refusal to solve a contact problem that is very actual for the numerous multivariant computations for different regimes of loading and the crystallographic orientations. One of the aims of the investigations was the selection of the equivalent (effective) length of the sample for the simplified formulation. The validity of the simplified formulation is based on the comparison with the results of full-scale formulation (with taking into account equipment), as well as on the comparison with the relative displacements of two markers measured in experiments.
In the general case there is no symmetry in the problem (see Fig.4 a) due to anisotropy of mechanical properties of single crystal sample. However in the important for practice case of [001] crystallographic orientation of sample the symmetry in respect to planes xz and yz (see Fig.4 b) can be introduced. Equipment and bolts were modeled by linear elastic material (steel), and for the sample the elasto-viscoвГУplastic model of the material was used.

The problem was solved in a three-dimensional, quasi-static formulation. As boundary conditions the symmetry conditions were set: zero displacements on the y-axis on the xz plane and zero displacements on the x-axis on the yz plane. On the lower side of the equipment zero displacements along the x and z axes were set. On the bolt cap the pressure of 100 MPa has been applied that is equivalent to the tightening force of the bolt. The mechanical properties for the alloys VZhM4 and VIN3 were taken from the papers [11, 12] and for ZhS32 from [2] (see Table 2 for details). The mechanical properties of bolts are taken for pearlitic steel [13].

Table 2. Mechanical properties of VZhM4 used in simulations [11]:

T	$^{\circ}C$	20	700	900	1000	1050
E_{001}	MPa	130000	96000	91000	86000	82000
ν	-	0.39	0.422	0.425	0.428	0.43
α	1/K	$1.1 \cdot 10^{-5}$	$1.7 \cdot 10^{-5}$	$1.9 \cdot 10^{-5}$	$2.1 \cdot 10^{-5}$	$2.3 \cdot 10^{-5}$
${\sigma_Y}^{001}$	MPa	846	950	-	-	820
n	-	8	8	8	8	8
A	$MPA^{-n}c^{-1}$	$1 \cdot 10^{-42}$	$1 \cdot 10^{-29}$	$1 \cdot 10^{-28}$	$2 \cdot 10^{-27}$	$1 \cdot 10^{-26}$

In simplified formulation (see Fig. 5 d) we consider only the sample without equipment, in which zero displacements on the symmetry planes xz and yz were set, the outer face of the sample parallel to the symmetry plane xz was fixed in the direction of the axis x. To exclude solid body motions, a number of points on this face were also fixed in the direction of the y and z axes.

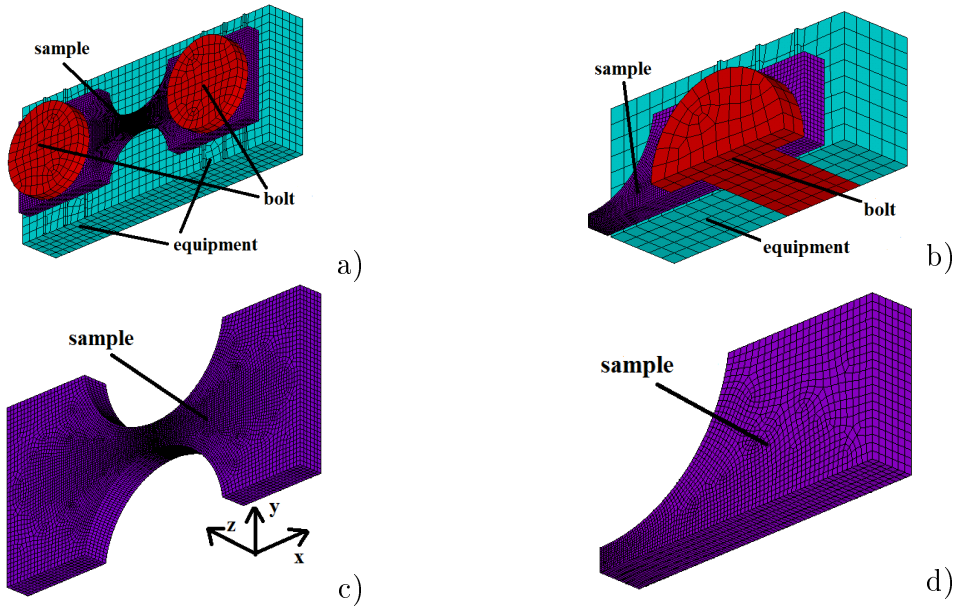

Figure 5: Finite-element models in mechanical problem: a) complete model (sample/bolt/equipment) without symmetry account, b) complete model (sample/bolt/equipment) with symmetry account, c) simplified model (sample only) without symmetry account, d) simplified model (sample only) with symmetry account.

Fig. 6 shows distributions of plastic strain intensity for nickel superalloys and three temperature modes after 7 cycles for thermoplasticity problem in ANSYS

(for VZHM4 and VIN3 the length of the sample is 42 mm, for ZHS32 is 50 mm).

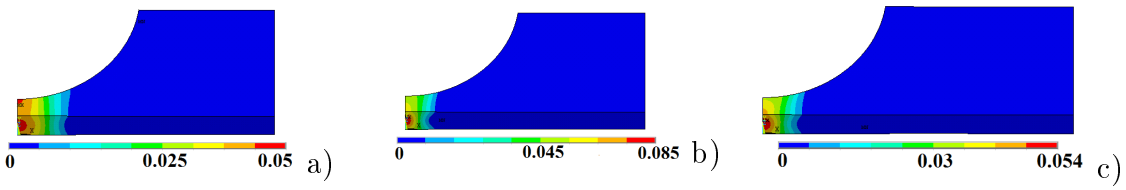

Figure 6: Distributions of plastic strain intensity for a) superalloy VZhM4, mode $700 \div 1050°C$; b) superalloy VIN3, mode $500 \div 1050°C$; c) superalloy ZhS32, mode $150 \div 900°C$ after 7 cycles.

The Table 6 shows the equivalent (effective) length of the sample for the simplified formulation, which has been found from the condition of equality of the inelastic strain ranges with complete model for different alloys. In the FE simulations with acceptable engineering accuracy can be used the value 40 mm. Effective length takes into account the compliance of equipment and its variation in considered range has no appreciable on the results.

Table 6. The equivalent length of the corset sample for different alloys.

VZhM4	VIN3	ZhS32
34-42 mm	38-46 mm	40-52 mm

4 Influence of delay on the thermal fatigue durability

Simulations of inelastic cyclic deformation of corset samples were performed by means of the FE program PANTOCRATOR [8], which allows to use the micromechanical (physical) models of plasticity and creep for single crystals [9, 10]. The Norton power-type law without hardening was applied to describe creep properties. The micromechanical plasticity model accounting 12 octahedral slip systems with lateral and nonlinear kinematic hardening [9] was used in the FE computation for single crystal alloy.

FE computations were carried out for a part of a corset sample (simplified FE model with effective length of sample equal 40 mm, see Fig. 7a.

The influence of the delay at maximum temperature on the number of cycles to the formation of macro cracks is analyzed in the range from 1 min to 1 hour for the cyclic loading regimes (see, for example, Fig. 7b) with:

- maximum temperature of $1000°C$ and a temperature range of $350°C$ and $550°C$;
- maximum temperature of $1000°C$ and a temperature range of $750°C$;
- maximum temperature of $900°C$ and a temperature range of $750°C$.

The heating times in the cycle were 7s, 25s, 18 s and 28s, the cooling time was 15s, 17s, 40s and 52s for VZhM4. The heating time in the cycle was 25 s, the cooling

time was 17s for VIN3. The heating times in the cycle was 25 s and 15s, the cooling time was 15s and 75s for ZhS32. The mechanical properties for the alloys VZhM4 and VIN3 were taken from the papers [11, 12] and for ZhS32 from [2].

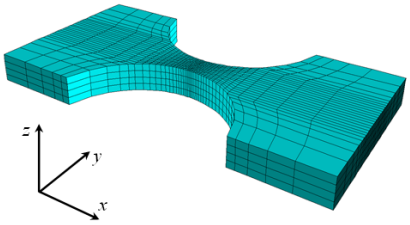

a)

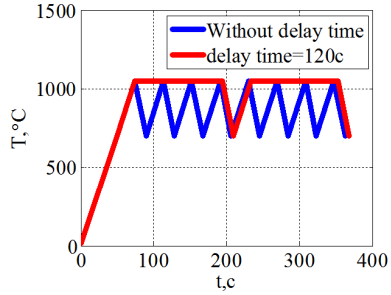

b)

Figure 7: a) Finite element model of sample (simplified formulation) for analysis of delay influence;b) temperature evolutions in central point of sample with and without delay for temperature regime 700-1050 $°C$

Damage calculation and estimation of the number of cycles before the formation of macrocracks were made on the basis of deformation four-member criterion [3],[4],[5]:

$$D = \sum_{i=1}^{N} \frac{\left(\Delta\varepsilon_{eq_i}^{p}\right)^{k}}{C_1(T)} + \sum_{i=1}^{N} \frac{\left(\Delta\varepsilon_{eq_i}^{c}\right)^{m}}{C_2(T)} + \max_{0\le t\le t_{max}} \frac{\varepsilon_{eq}^{p}}{\varepsilon_r^{p}(T)} + \max_{0\le t\le t_{max}} \frac{\varepsilon_{eq}^{c}}{\varepsilon_r^{c}(T)}, \tag{3}$$

where the first term takes into account the range of plastic strain within the cycle, the second term is the range of creep strain within the cycle, the third term is unilaterally accumulated plastic strain (ratcheting), the fourth term is unilaterally accumulated creep strain. The number of cycles before the formation of macrocracks N is determined from the condition D = 1. The maximum shear strain in the sliding system with normal to the slip plane n and the sliding direction l is considered as equivalent deformation. The values k=2, m = 5/4 , $C_1 = (\varepsilon_r^p)^k$, $C_2 = 3/4 * (\varepsilon_r^c)^m$ are usually accepted, where ε_r^p and ε_r^c ultimate strains of plasticity and creep under uniaxial tension.

In the FE computations the values of ultimate strain $\varepsilon_r^p = 0.40$ for VZhM4, $\varepsilon_r^p = 0.36$ for ZhS32, $\varepsilon_r^p = 0.42$ for VIN3 were used. Improvement of the accuracy of prediction of influence the delay time on durability can be achieved by the refinement of the constant ε_r^p on the basis of data without delay.

The comparison of the results of FE simulations and experiments concerning the effect of the delay time at the maximum temperature on the thermal fatigue durability for single-crystal superalloys VZhM4, VIN3 and ZhS32 is given in Fig. 8,9,10.

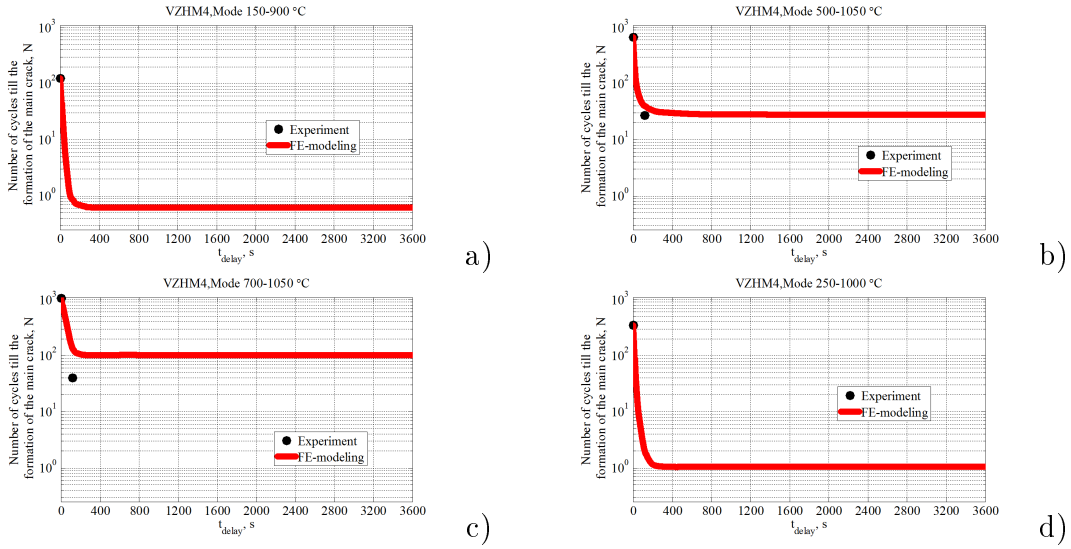

Figure 8: Comparison of results of FE simulation and experimental data for the alloy VZhM4: a)mode $150 \div 900°C$, heating time is 28s, cooling time is 52s,b)mode $500 \div 1050°C$, heating time is 7s, cooling time is 15s,c)mode $700 \div 1050°C$ heating time is 25s, cooling time is 17s,d)mode $250 \div 1000°C$ heating time is 18s, cooling time is 40s.

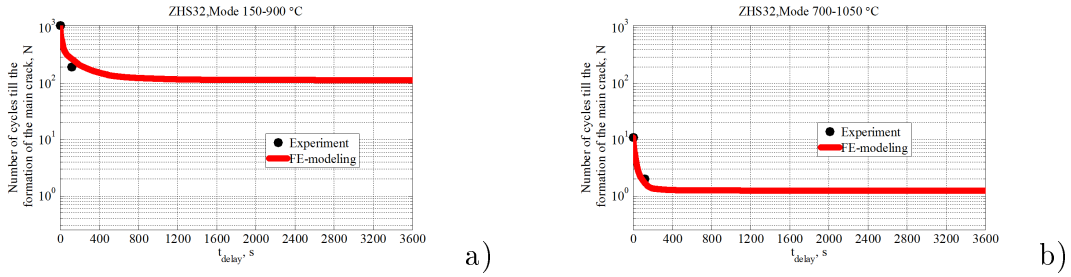

Figure 9: Comparison of results of FE simulation and experimental data for alloy ZhS32: a) mode $150 \div 900°C$, heating time is 25 s, cooling time is 75 s, b) mode $700 \div 1050°C$, heating time is 15 s, cooling time is 15 s.

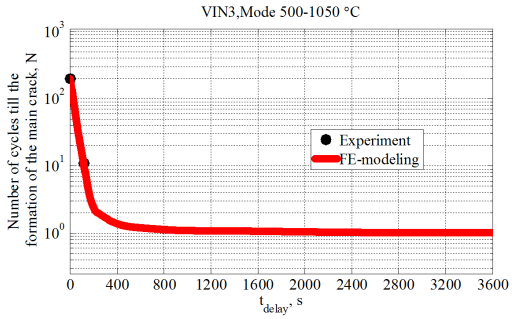

Figure 10: Comparison of calculation and experiment for alloy VIN3, mode 500-1050 $°C$, heating time-25 s, cooling time-17s

5 Conclusions

The results of the computations show a good agreement with the experiment, which suggests that the finite-element computations in combination with application of deformational criterion can be used to predict the thermal-fatigue strength of various single-crystal superalloy samples in wide range temperatures.

Acknowledgements

The study was performed under financial support of RFBR grant No. 16-08-00845 and scholarship program Siemens.

References

[1] Shalin R.E., Svetlov I.L., Kachalov E.B. and other Single crystals of nickel heat-resistant alloys-M.: Mashinostroenie, 1997. - 336 p.

[2] Getsov L. B. Materials and strength of gas turbine parts.-Rybinsk: Publishing House Gas Turbo Technology. 2010- 2011

[3] Getsov L. B., Semenov A. C. Criteria of fracture of polycrystalline and single crystal materials under thermal cyclic loading // Proceedings of CKTI. Vol. 296, 2009, pp. 83-91.

[4] Semenov A.S., Getsov L.B. Thermal fatigue fracture criteria of single crystal heat-resistant alloys and methods for identification of their parameters // Strength of Materials, 2014. Vol. 46, No. 1, p. 38-48.

[5] Getsov L.B., Semenov A.S., Staroselsky A. A failure criterion for single-crystal superalloys during thermocyclic loading // Materials and technology. 2008. Vol. 42, P. 3вГУ12.

[6] Petrushin N. Oh. Logunov A.V., Kovalev A. I., Zverev A. F., Toropov V. M., Fedotov N. H. Thermophysical properties of Ni_3Al-Ni_3Nb directly crystallized eutectic composition / / High temperature thermophysics, 1976, вНЦ 3.

[7] May S., Semenov A.S. Modeling of inelastic cyclic deformation of monocrystalline specimens // Proc. of the XXXIX week of science of SPbGPU. 2010. Vol. 5. P. 73-74.

[8] Semenov A. S. PANTOCRATOR is a finite-element software package focused on solving nonlinear problems of mechanics / Proceedings of the V-th International. Conf. "Scientific and technical problems of forecasting reliability and durability of structures". SPb.: Izd-vo SPbSPU, 2003. p. 466-480.

[9] Cailletaud G.A. Micromechanical approach to inelastic behaviour of metals // Int. J. Plast., 1991, 8, p. 55-73.

[10] A. S. Semenov. Identification of anisotropy parameters of phenomenological plasticity criterion for single crystals on the basis of micromechanical model // Scientific and technical sheets SPbGPU. Physical and mathematical Sciences. 2014. No. 2 (194). p. 15-29.

[11] Kablov E. N., Petrushin N. O. Svetlov I. L., Demonis I. M. Nickel casting heat-resistant alloys of the new generation. The jubilee nauch.- tech. sat. Aviation materials and technologies. M: Proceedings of VIAM 2012, p. 36-52.

[12] Semenov S. G., Getsov L. B., Semenov A. S., Petrushin N. V., Ospennikova O. G., A. A. Zhivushkin The issue of enhancing resource capabilities of nozzle blades of gas turbine engines through the use of new single crystal alloy // Journal of Machinery Manufacture and Reliability. 2016. No.4, p.30-38.

[13] Zinoviev V.E., Thermo-physical properties of metals at high temperatures. Moscow: Metalurgia, 1989.

[14] Chirkin V.S. Thermophysical properties of nuclear materials. Moscow:Atomizdat, 1968, p. 161.

[15] Maslenkov S.B., Maslenkova E.A. Steels and alloys for high temperatures. Moskow: Metallurgia, 1991.

Artem V. Savikovskii,SPbSPU,Politechnicheskaya 29;195251,St.Petersburg,Russia
Artem S. Semenov,SPbSPU,Politechnicheskaya 29;195251, St.Petersburg, Russia
Leonid B. Getsov,NPO CKTI,Politechnicheskaya 24;194021,St. Petersburg,Russia